World Journal of Pharmaceutical Science and Research

www.wjpsronline.com

Research Article

ISSN: 2583-6579
SJIF Impact Factor: 6.916
Year - 2026
Volume: 5; Issue: 6
Page: 841-854

IN SILICO DESIGN AND EVALUATION OF NOVEL BENZOXAZINE DERIVATIVES AS POTENTIAL CDK9 INHIBITORS FOR ANTICANCER THERAPY

Namrata Ravba Jaybhaye*, Dr. Atul N. Khadse, Vaishnavi R. Agrawal

PRES's College of Pharmacy (for women) Chincholi, Sinnar Dist. Nashik Maharashtra.

Article Received: 18 April 2026 | | ***Article Revised: 08 May 2026*** | | ***Article Accepted: 29 May 2026***

***Corresponding Author: Namrata Ravba Jaybhaye**
PRES's College of Pharmacy (for women) Chincholi, Sinnar Dist. Nashik Maharashtra.
DOI: https://doi.org/10.5281/zenodo.20688677

How to cite this Article: Namrata Ravba Jaybhaye, Dr. Atul N. Khadse, Vaishnavi R. Agrawal (2026) IN SILICO DESIGN AND EVALUATION OF NOVEL BENZOXAZINE DERIVATIVES AS POTENTIAL CDK9 INHIBITORS FOR ANTICANCER THERAPY. World Journal of Pharmaceutical Science and Research, 5(6), 841-854.

ABSTRACT

Cyclin-Dependent Kinase 9 (CDK9) is a crucial regulator of tumour cell proliferation, survival, and oncogenic gene expression. Transcriptional dysregulation is a known hallmark of cancer. In this work, a novel series of compounds containing benzoxazine was designed and evaluated in silico as possible therapeutic drugs that target CDK9. To evaluate the binding affinities and interaction patterns of ten proposed compounds (1–10) with the CDK9 enzyme (PDB ID: 6GHZ), molecular docking studies were conducted using AutoDock and AutoDock Vina. With binding affinities of −9.0 kcal/mol and −8.8 kcal/mol, respectively, Compound 6 and Compound 4 outperformed the standard medication CDK9-IN-23 (−8.2 kcal/mol) among the series. Additionally, a physicochemical study and in silico ADMET showed that most of these substances adhere to Lipinski's rule of five, having acceptable pharmacokinetic characteristics and no anticipated AMES toxicity. These results demonstrate the benzoxazine scaffold's potential as a viable lead for targeted anticancer treatment.

KEYWORDS: Benzoxazine, CDK9, Anticancer activity, Transcriptional regulation, Molecular docking, In-Silico ADMET.

1. INTRODUCTION

Cancer is a complicated, multifactorial illness marked by aberrant cellular metabolism, resistance to apoptosis, and unchecked cell proliferation. The dysregulation of transcriptional mechanisms, which results in the ongoing expression of genes involved in cell survival and metastasis, is a key factor in the etiology of cancer.[1] Targeting transcriptional regulators has become a viable oncology therapy in recent years. The primary catalytic element of the positive transcription elongation factor b (P-TEFb) complex is cyclin-dependent kinase 9 (CDK9), a serine/threonine kinase.

CDK9 facilitates the shift from transcription initiation to productive elongation by phosphorylating the C-terminal domain of RNA polymerase II and negative elongation factors in conjunction with cyclin T.[2,3] mechanism is necessary for cancer cells to express short-lived antiapoptotic and carcinogenic proteins (such MYC and MCL-1). As a result, CDK9 is a very desirable target for anticancer therapy because overactivation of CDK9 results in persistent transcription of survival genes.[4]

In the field of pharmaceutical sciences, benzoxazines constitute a prominent class of fused bicyclic heterocyclic molecules.[5] Benzoxazine derivatives have a variety of biological actions, including strong antibacterial and anticancer effects, due to their structurally advantageous framework. Using molecular docking and pharmacokinetic prediction, ten benzoxazine-based derivatives were designed and assessed as possible CDK9 inhibitors in this work using Computer-Aided Drug Design (CADD).[6,7]

2. MATERIALS AND METHODS

2.1. Software and Tools: Molecular modelling and structural analyses were conducted using a suite of computational tools:

- ChemDraw 8.0: For 2D structure drawing and geometric arrangement.[8,9]
- AutoDock Tools & AutoDock Vina: For automated protein-ligand docking simulations.[10]
- Open Babel: For chemical file format conversion (PDB to PDBQT).[11]
- SwissADME: For predicting drug-likeness and physicochemical parameters.[12,13]
- PyMOL: For 3D visualization and interaction analysis of protein-ligand complexes.[14,15]

2.2. Protein Preparation

The RCSB Protein Data Bank provided the human CDK9 3D crystal structure (PDB ID: 6GHZ, Resolution: 2.33 Å). Water molecules and heteroatoms (co-crystallized ligands) were removed during preparation, and polar hydrogens and Kollman charges were then added. The coordinates of the docking grid box were X: 35.295, Y: 8.045, Z: 10.03, with a spacing of 0.375 Å and measurements of 40x40x40 Å.[10,11]

2.3. Ligand Preparation

ChemDraw was used to develop ten new benzoxazine compounds (Compounds 1–10) and the conventional inhibitor (CDK9-IN-23). In order to provide appropriate bond rotation parameters for flexible docking, structures were energetically reduced and transformed into the PDBQT format using Open Babel.[10,11]

2.4. Rational Design Strategy

In order to optimize interaction within the catalytic domain of CDK9, different functional groups were substituted in the design of these derivatives, which were based on a benzoxazine core scaffold. To improve hydrophobic and hydrogen-bonding interactions with important active-site residues such GLN72, ILE85, and ARG11, different electronegative groups, sulfonamides, and cyclic substitutions were specifically added.[4,5]

3. RESULTS AND DISCUSSION

3.1. Molecular Docking Analysis

Docking simulations revealed that several redesigned benzoxazine derivatives bound effectively to the catalytic active site of CDK9, many outperforming the standard reference drug.[16].

Table 1: Binding Affinities and Key Residue Interactions for CDK9 (PDB ID: 6GHZ).

Compound	Dock Score (kcal/mol)	Key Amino Acid Interactions
CDK9-IN-23 [Std]	-8.2	ARG11, GLU147, ILE85, GLN72, PHE13, GLY145, ASN9, ILE83
Compound 1	-8.7	GLU84, GLN72, ASN8, ARG11, GLU147, GLY145, ARG68, ILE85
Compound 2	-6.5	ARG254, ASN180, THR179, PHE176, ILE255
Compound 3	-8.7	GLY145, PHE13, ILE85, ARG11, THR149, GLN72
Compound 4	-8.8	THR149, GLU147, GLN72, LYS75, ILE85, GLY145
Compound 5	-8.6	ILE85, GLN72, LYS75, GLY145, PHE13, ARG11
Compound 6	-9.0	LYS75, LEU82, GLN72, ILE83, ILE85, ARG11, PHE13
Compound 7	-8.1	PHE13, GLY145, PHE146, GLN72, ILE85, CYS14, GLU84, LYS75
Compound 8	-8.1	1LYS75, ILE85, GLN72, GLU147, ARG68, TYR13
Compound 9	-7.7	ILE83, GLU84, ILE85, GLN72, ARG11, GLU147, PHE13, LEU148
Compound 10	-8.4	GLN72, THR149, ASN9, ASN8, ARG11, GLU147, TRP12, ARG88
Compound 11	-7.4	THR149, GLU147, ILE85, ILE83, LYS75, LEU82, GLU84
Compound 12	-7.6	GLU84, ILE85, ARG11, LEU82, GLN72, GLU147
Compound 13	-8.2	ARG11, GLU147, GLN72, ILE85, GLU, LEU82
Compound 14	-7.4	ASN8, THR149, GLU147, GLN72, LEU38, ARG66, ARG11
Compound 15	-7.5	ARG11, GLU147, LEU82, GLU84, GLN72, ILE85

Molecular Docking

- **Docking of molecular Structure**

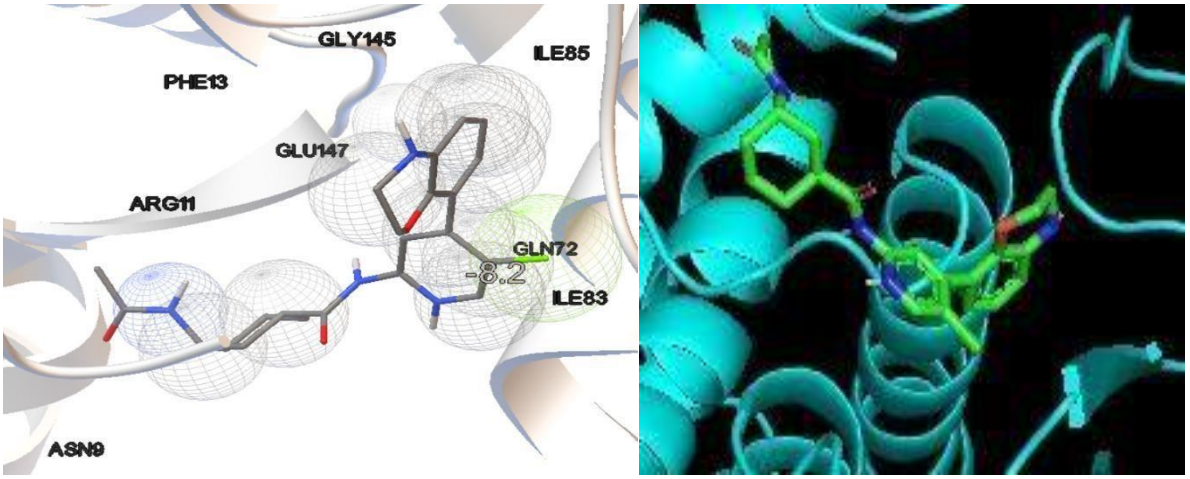

Fig. 1: Binding interaction of CDK9-IN-23[Standard] (-8.2 Kcal/mol).

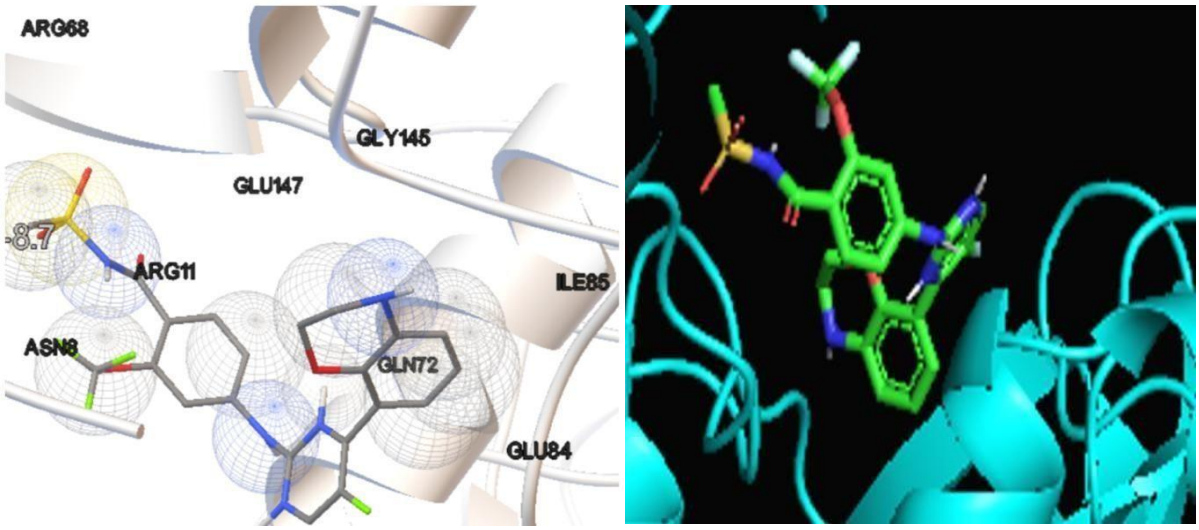

Fig. 2: Binding interaction of Compound 1 (-8.7 Kcal/mol).

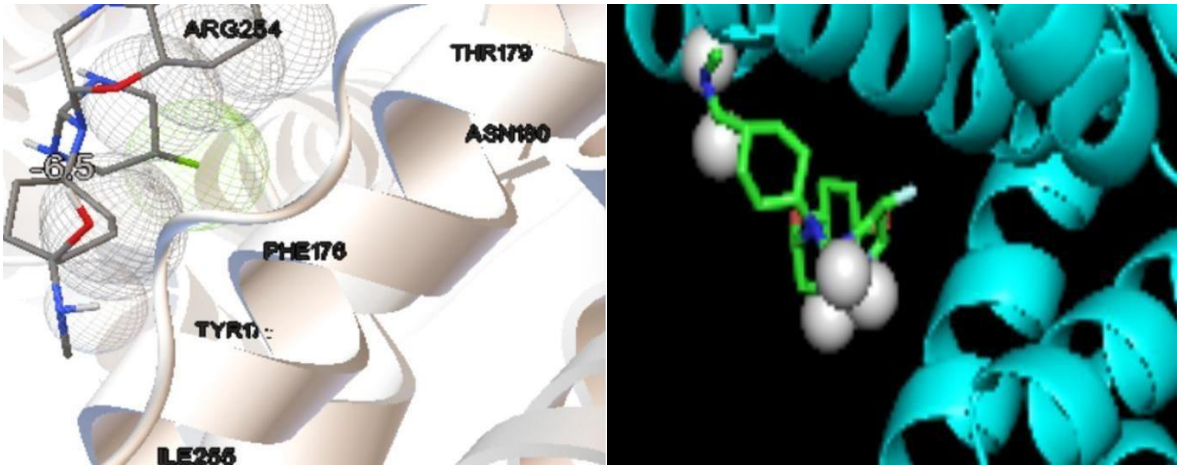

Fig. 3: Binding interaction of Compound 2 (-6.5 Kcal/mol).

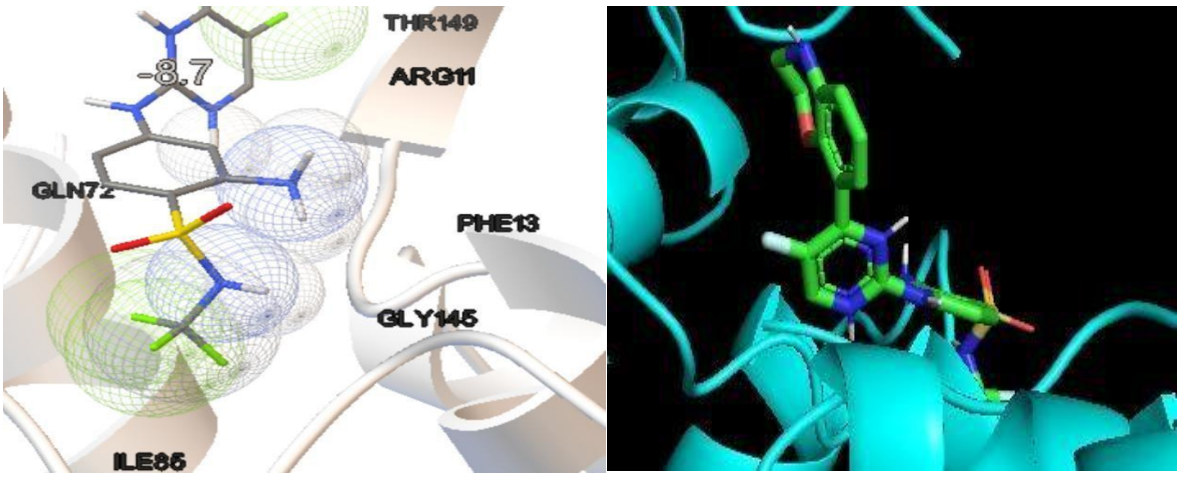

Fig. 4: Binding interaction of Compound 3 (-8.7 Kcal/mol).

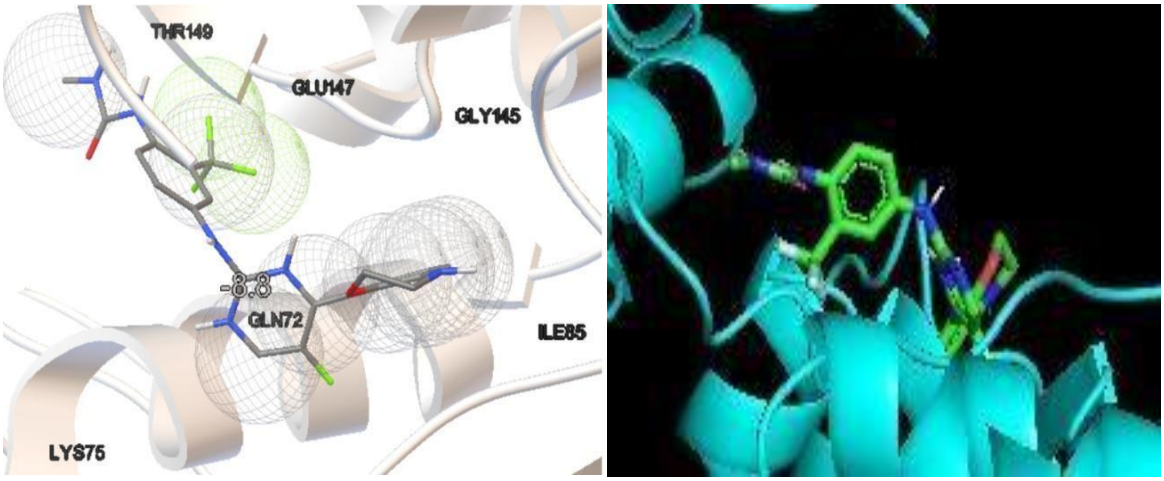

Fig. 5: Binding interaction of Compound 4 (-8.8 Kcal/mol).

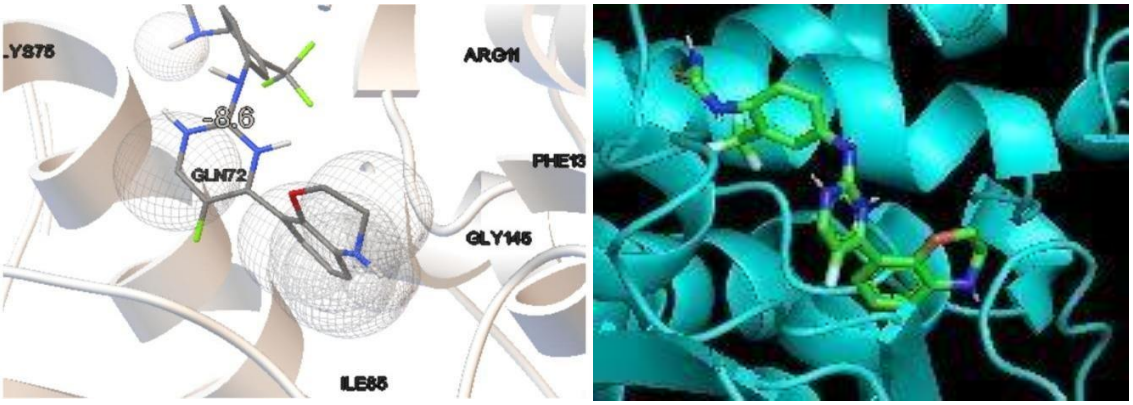

Fig. 6: Binding interaction of Compound 5 (-8.6 Kcal/mol).

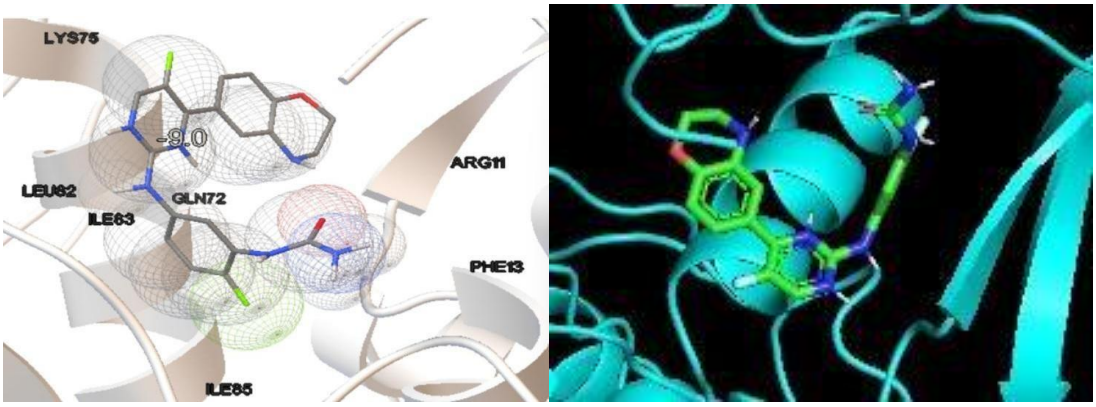

Fig. 7: Binding interaction of Compound 6 (-9.0 Kcal/mol).

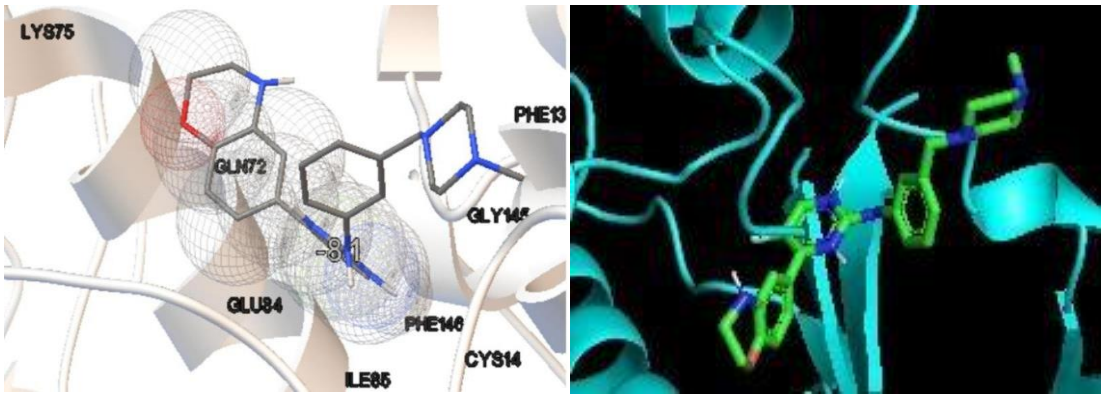

Fig. 8: Binding interaction of Compound 7 (-8.1 Kcal/mol).

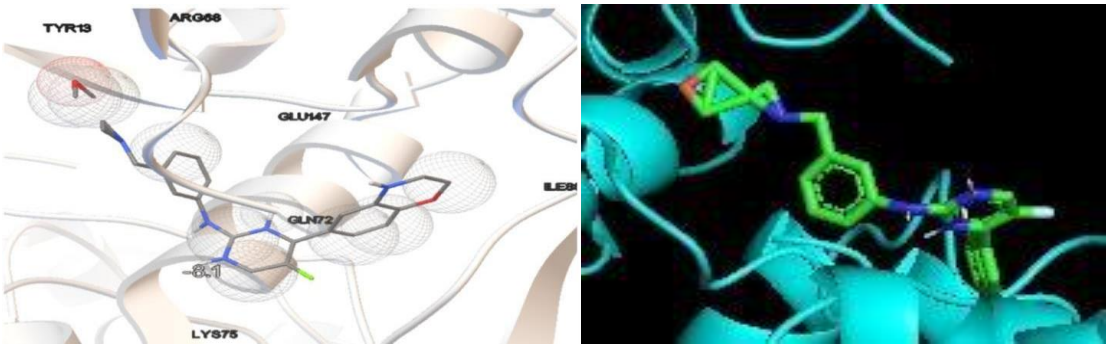

Fig. 9: Binding interaction of Compound 8 (-8.1 Kcal/mol).

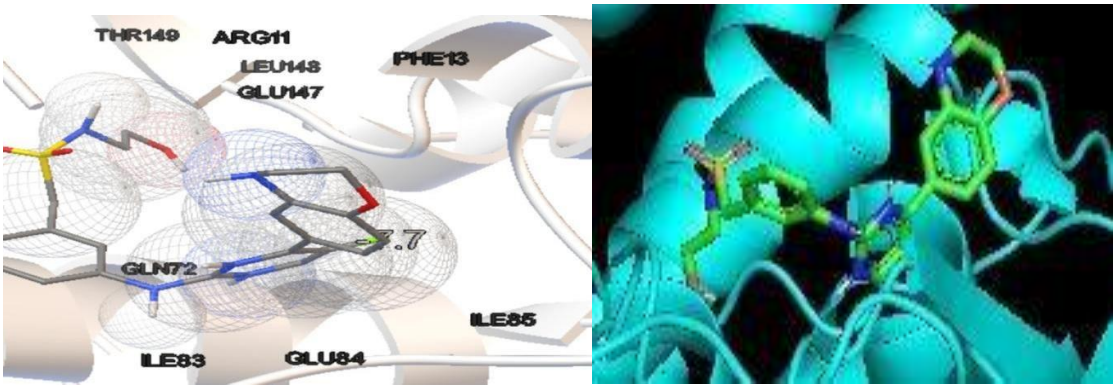

Fig. 10: Binding interaction of Compound 9 (-7.7 Kcal/mol).

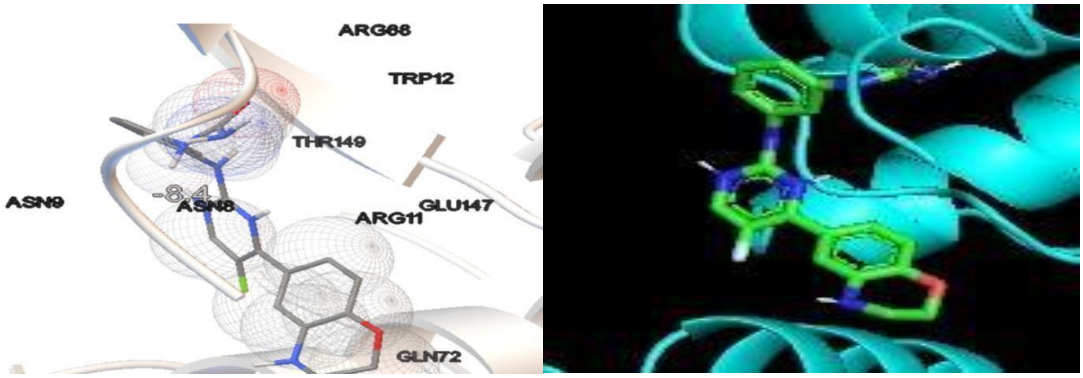

Fig. 11: Binding interaction of Compound 10 (-8.4 Kcal/mol).

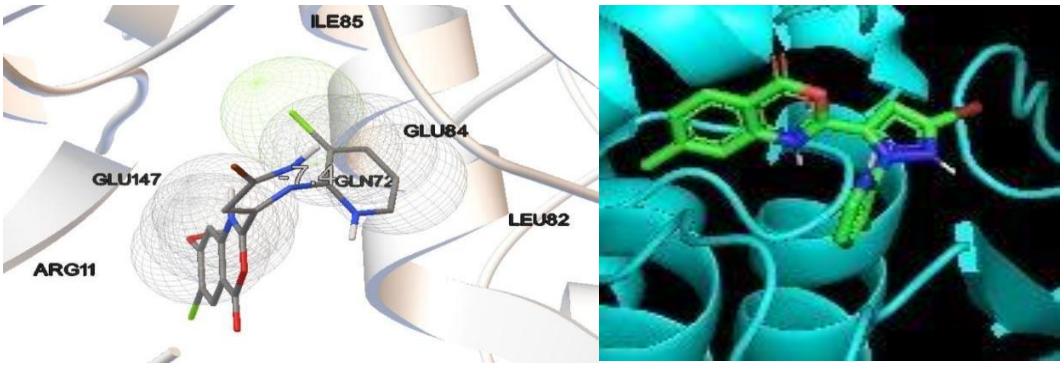

Fig. 12: Binding interaction of Compound 11 (-7.4 Kcal/mol).

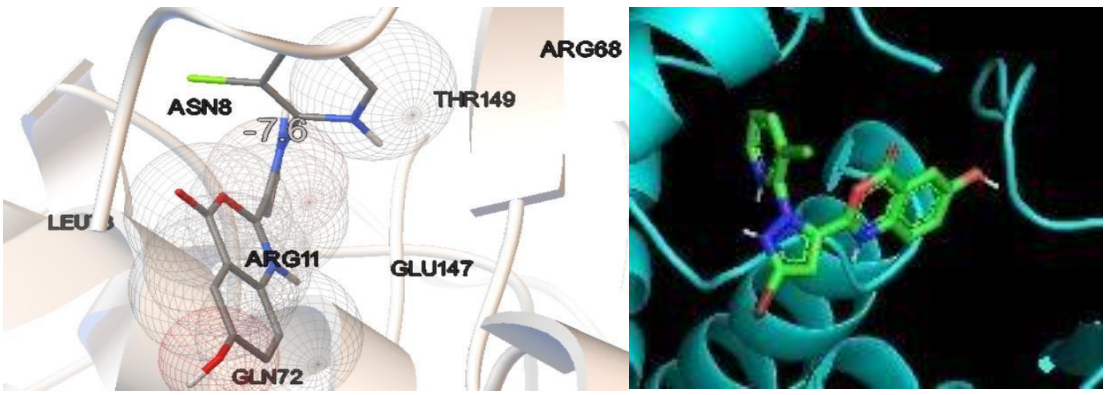

Fig. 13: Binding interaction of Compound 12 (-7.6 Kcal/mol).

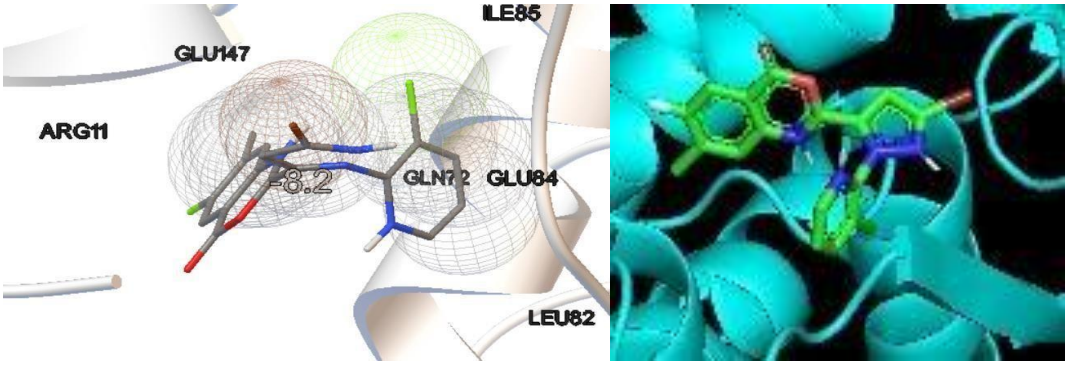

Fig. 14: Binding interaction of Compound 13 (-8.2 Kcal/mol).

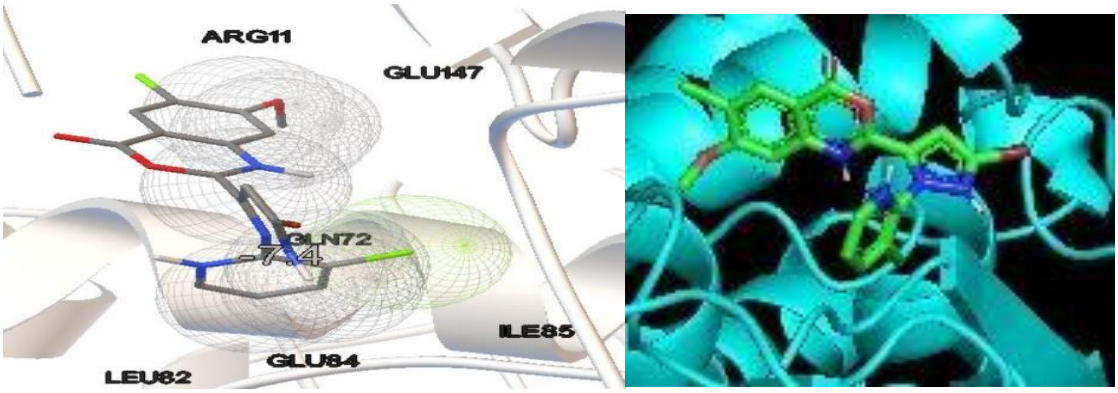

Fig. 15: Binding interaction of Compound 14 (-7.4 Kcal/mol).

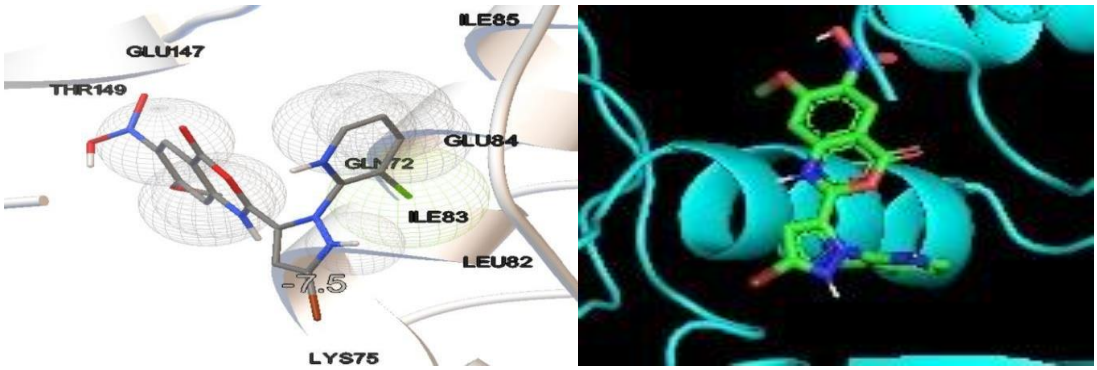

Fig. 16: Binding interaction of Compound 15 (-7.5 Kcal/mol High)

Affinity Leads (Compound 6,4,1,3)

At −9.0 kcal/mol, compound 6 showed the highest binding affinity. Strong electronegative groups (fluorines) and a main amide were coupled with the benzoxazine core to generate extremely stable hydrogen bonding networks and pi-pi stacking interactions with LYS75, GLN72, and ILE85. Compound 4, which effectively used GLU147 and THR149 to stabilize the complex, trailed closely at −8.8 kcal/mol.[16,17]

Moderate-Affinity Compounds

The binding affinities of compounds 5, 10, 7, 14, and 8 (-8.6 to -8.1 kcal/mol) were either somewhat better than or equal to the standard. In contrast to the top leads, they encountered minor steric constraints but successfully anchored within the active site.

Lowest-Affinity Compound

Compound 2, which interacted with a different set of residues (ARG254, THR179), scored lower (-6.5 kcal/mol), indicating a binding orientation that results in a larger entropic penalty in the targeted catalytic pocket.

3.2. Physicochemical and Drug-likeness Profiling

The proposed benzoxazine compounds largely follow Lipinski's rule of five, indicating good potential for oral bioavailability, according to pharmacokinetic evaluation using SwissADME.[12,13]

Table 2: In Silico Physicochemical and ADME Properties.

Compound	MW(g/mol)	Rotatable Bonds	H-Bond Acceptors	H- Bond Donors	TPSA (Å²)	Lipinski/ Violations
Standard	428.91	30*	12	3	92.35 Å²	Yes: 0 violation
Compound 1	462.40	7	8	4	100.20 Å²	Yes: 0 violation
Compound 2	409.41	6	6	2	88.61 Å²	Yes: 0 violation
Compound 3	527.45	8	6	3	39.92 Å²	Yes: 0 violations
Compound 4	527.45	8	11	3	39.92 Å²	Yes: 0 violation
Compound 5	383.35	4	11	3	102.16 Å²	Yes: 0 violation
Compound 6	398.37	5	6	4	114.19 Å²	Yes: 0 violation
Compound 7	434.51	5	6	2	65.55 Å²	No:1 violation
Compound 8	421.47	5	6	2	71.54 Å²	Yes:0 violation
Compound 9	459.49	8	8	4	33 .85 Å²	No:1 violation
Compound0	380.38	5	5	4	114.19 Å²	Yes:0 violation
Compound 11	418.65	2	5	0	80.71 Å²	Yes:0 violation
Compound 12	419.62	2	6	1	94.04 Å²	Yes:0 violation
Compound 13	436.64	2	6	0	80.71 Å²	Yes:0 violation
Compound 14	469.10	3	6	0	89.94 Å²	Yes:0 violation
Compound 15	479.65	4	8	1	132.70 Å²	Yes:0 violation

The strongest inhibitor, compound 6, supported favorable cell permeability with an ideal TPSA of 114.19 Å², a molecular weight of 398.37 g/mol, and an outstanding physicochemical profile with zero Lipinski violations.

3.3. Toxicity Prediction

One major obstacle to early-stage medication development is toxicity. To forecast possible clinical viability, the synthesized compounds' expected safety profile was assessed.

Table 3: Predicted Toxicity Parameters.

Compound	Bioavailability Score	AMES Toxicity	Hepatotoxicity	Skin Sensitization
Standard	0.55	No	Yes	No
Compound 1	0.55	No	Yes	No
Compound 2	0.55	No	Yes	No
Compound 2	0.55	No	Yes	No
Compound 3	0.55	No	Yes	No
Compound 4	0.55	No	Yes	No
Compound 5	0.55	No	Yes	No
Compound 6	0.55	No	Yes	No
Compound 7	0.55	No	Yes	No
Compound 8	0.55	No	Yes	No
Compound 9	0.55	No	Yes	No
Compound 10	0.55	No	Yes	No
Compound 11	0.55	No	Yes	No
Compound 12	0.55	No	Yes	No
Compound 13	0.55	No	Yes	No

Compound 14	0.55	No	Yes	No
Compound 15	0.55	No	Yes	No

All 10 of the target compounds had a typical oral bioavailability score of 0.55. It is quite comforting that there was no skin sensitization or AMES toxicity over the entire series. The expected hepatotoxicity is a common warning indication for kinase inhibitors and emphasizes the necessity for focused administration or structural modification in subsequent rounds.

3.4. In vitro Biological Evaluation (Proposal)

Based on the in-silico results, Compounds 6, 4, 1, and 3—the most potent benzoxazine derivatives—are chosen for in vitro biological testing. To ascertain their inhibitory capability, these substances should first be examined utilizing CDK9 enzyme inhibition tests. Additionally, the MTT assay should be used to assess cytotoxic activity on cancer cell lines such as HeLa or HL-60. Further research, including apoptosis detection, cell cycle arrest analysis, and gene expression investigations (MYC and MCL-1 proteins), should be carried out to comprehend their process. Strong docking scores, negligible AMES toxicity, and good drug-likeness demonstrated the compounds' suitability for biological testing. Due to its strong contact with important CDK9 residues and maximal binding affinity of -9.0 kcal/mol, Compound 6 is predicted to have the highest activity of all.[18,19]

3.5. Structure-Activity Relationship (SAR)

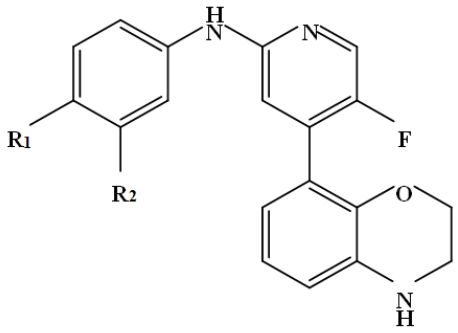

i. Benzoxazine Core (Pharmacophore Region)

As the main pharmacophore, the benzoxazine core is crucial in defining the compounds' biological action. In the CDK9 active site, it facilitates hydrophobic interactions and π–π stacking with amino acid residues like ILE85 and PHE13. By boosting lipophilicity and stabilizing interactions inside the binding pocket, halogen substituents on this core further improve activity. Due to strong interactions with residues like LYS75, ILE85, and GLN72, Compound 6 (−9.0 kcal/mol) showed the highest activity, followed by Compound 4 (−8.8 kcal/mol). Docking scores are significantly lower for compounds with weaker interaction patterns, underscoring the significance of this fundamental structure.[19,20]

Phenyl Ring Substitution (R^1, R^2 Region)

The biological activity of the benzoxazine derivatives is greatly affected by substitution on the phenyl ring, which modifies hydrophobic and electrical interactions. By increasing penetration into the hydrophobic pocket of CDK9 and fortifying ligand–protein interactions, the presence of tiny electron-withdrawing groups like fluorine and chlorine at the R^1 and R^2 locations improves binding affinity. Compound 6 (−9.0 kcal/mol), Compound 4 (−8.8 kcal/mol), and Compounds 1 and 3 (−8.7 kcal/mol) are examples of high-activity compounds where halogen substitution led to better

docking scores. Conversely, compounds with poor orientation or inadequate substitution, like Compound 2 (−6.5 kcal/mol), showed markedly decreased activity because of weaker contacts and poor fitting inside the active site.[1,9,20]

ii. Linker Region (–NH– Bridge)

A crucial structural element that is vital to sustaining biological activity is the –NH– linker. It stabilizes the ligand inside the CDK9 binding pocket by acting as a hydrogen bond donor and facilitating important interactions with hinge area residues, especially GLN72. Strongly active compounds, like Compounds 6 and 4, preserve this linker and create stable hydrogen bonding networks, leading to high binding affinities of −9.0 and −8.8 kcal/mol, respectively. Since appropriate molecular orientation and interaction heavily depend on this functional group, any disruption or change of this linker would probably decrease hydrogen bonding capability and adversely influence activity.[20]

iv. Pyrimidine Ring (Hinge Binding Region)

As the hinge-binding moiety, the pyrimidine ring is crucial for anchoring the molecule inside CDK9's ATP-binding site. Strong interactions with important residues like GLN72 and ARG11 are made possible by its nitrogen atoms acting as hydrogen bond acceptors. Through these interactions, compounds with optimal binding, such as Compound 6 (−9.0 kcal/mol) and Compound 3 (−8.7 kcal/mol), exhibit effective hinge binding, which contributes to their increased activity. Conversely, Compound 2 (−6.5 kcal/mol) interacts with noncritical residues (such ARG254 and THR179), indicating less hinge interaction and incorrect binding orientation, which ultimately reduces its inhibitory potential.[19,20]

The SAR of this benzoxazine series that targets CDK9 can be further understood by analyzing the docking scores and chemical structures:

Halogenation Enhances Binding

Compared to unsubstituted versions, the incorporation of strongly electronegative elements, especially fluorine atoms (as demonstrated in Compounds 6, 4, 1, and 3), greatly increased binding energies. These halogens create stable dipole contacts and enable deeper penetration into CDK9's hydrophobic region.[21, 22]

Hydrogen Bond Networks

The ligand-enzyme complex was effectively stabilized by compounds containing terminal amine or amide groups that might function as multi-directional hydrogen bond donors (e.g., Compound 6), particularly engaging with important hinge area residues like GLN72 and ARG11.

Table 4: Structural Substitutions and Corresponding Target Affinity.

Compound	R1-R2 Group Substitution	Electronic Nature	Dock Score	Structural and Binding Impact
Compound 1	R1: -NH- CO-NH- CH3 R2: -CF3	Electron withdrawing	-8.7	Halogen substitution improves hydrophobic fitting in the CDK9 pocket and supports stable interactions with GLU84, GLN72, ARG11, GLU147, GLY145, and ILE85, giving strong binding.
Compound 2	R1: -NH- CO-NH- CH3	Weakly favorable or poorly oriented electronic effect	-6.5	This compound binds in an improper orientation and interacts with noncritical residues such as ARG254, ASN180, and THR179, so its affinity is much lower than the active analogs.

Compound 3	R1: -SO2- NH-CF3 R2: -NH2	Electron withdrawing	-8.7	The electron-withdrawing substitution helps proper hinge-region anchoring and promotes favorable contacts with GLY145, PHE13, ILE85, ARG11, THR149 and GLN72.
Compound 4	R1: -CO- NH-SO2- CH3 R2: -OCF3	Electron withdrawing	-8.8	Strong substitution pattern favors interaction with GLU147, THR149, GLN72, LYS75, ILE85 and GLY145, leading to a highly stabilized complex.
Compound 5	R: $–CONH_2$ + Fluoro on phenyl	Mixed, moderately electron withdrawing	-8.6	Shows good pocket anchoring and maintains key contacts with ILE85, GLN72, LYS75, GLY145, PHE13 and ARG11, but with slightly less optimal fit than the best leads.
Compound 6	R: $–NH– CO–NH_2$ + Fluoro substitution on phenyl	Strongly electron withdrawing g with H-bonding character electronic effect	-9.0	This is the best compound. The substituents strengthen hydrophobic, dipolar and hydrogen-bonding interactions, especially with LYS75, LEU82, GLN72, ILE83, ILE85, ARG11 and PHE13.
Compound 7	R: $-CH_2–N(CH_3)–$ (piperazine ring)	Moderately electron-donating to neutral, with steric effect	-8.1	Binds reasonably well, but bulkier substitution likely creates slight steric restriction, reducing affinity compared with Compounds 4 and 6.
Compound 8	R: $–CH_2–$ Morpholine ring	Moderately electron donating to neutral	-8.1	Maintains acceptable active-site anchoring with LYS75, ILE85, GLN72 and GLU147, but does not optimize interactions as efficiently as the top compounds.
Compound 9	R: $–CH_2– SO_2–NH– CH_2–CH_2–OH$	Mixed electronic behaviour	-7.7	Retains some essential contacts with ILE83, GLU84, ILE85, GLN72, and ARG11, but weaker overall stabilization gives only moderate docking.
Compound 10	R: $–NH–CO–NH_2$	Electron withdrawing / polar	-8.4	Shows good hinge-region binding through GLN72, THR149, ASN9, ASN8, ARG11 and GLU147. The polar group helps binding, but not as strongly as Compound 6.
Compound 11	R1: –CH3 R2: -H	Weakly electron-withdrawing / neutral	-7.4	Maintains partial binding contacts, but reduced complementarity in the active site leads to lower affinity.
Compound 12	R1: $–CH(CH_3)_2$ R2: -H	Weakly electron-withdrawing	-7.6	Forms some useful contacts with GLU84, ILE85, ARG11, LEU82, GLN72 and GLU147, though the substitution is not strong enough to maximize binding
Compound 13	R1: -H R2: -OH	Electron withdrawing / neutral	-8.2	Gives binding comparable to the standard by maintaining hinge and hydrophobic pocket interactions with ARG11, GLU147, GLN72, ILE85, GLU84, and LEU82.
Compound 14	R1: -OCH3 R2: -NO2	Mostly neutral with steric penalty	-7.4	The compound interacts with ASN8, THR149, GLU147, GLN72, LEU38, ARG66, and ARG11, but binding is weakened by a less favorable orientation.
Compound 15	R1: -OCH3 R2: -Cl	Mixed polar electronic effect	-7.5	Shows moderate activity by preserving some key contacts, but steric and orientation issues reduce overall binding efficiency.

3.6. BOILED-Egg Predictive Model Analysis

Fig. 12: BOILED-Egg predictive model for the top-scoring benzoxazine derivatives (Compound 1,3,4,6) and the Standard compound is CDK9-IN-23.

The pharmacokinetic behaviour of the chosen benzoxazine derivatives (Compounds 1, 3, 4, and 6), in contrast to the conventional CDK9 inhibitor (CDK9-IN-23), was shown by the BOILED-Egg model and SwissADME analysis. The majority of the assessed compounds were located in the white area of the BOILED-Egg plot, indicating good gastrointestinal absorption. However, none of them significantly penetrated the yellow area, indicating low blood–brain barrier permeability—a useful characteristic for anticancer drugs to prevent side effects related to the central nervous system. With an appropriate TPSA (114.19 Å²) and a superior docking score (−9.0 kcal/mol), Compound 6 showed the best balance of lipophilicity and polarity among the series. It was followed by Compounds 4 (−8.8 kcal/mol), 1 (−8.7 kcal/mol), and 3 (−8.7 kcal/mol), all of which outperformed the standard (−8.2 kcal/mol). Although minor hepatotoxicity was seen, which is consistent with kinase inhibitors, SwissADME predictions further revealed that these drugs meet Lipinski's rule of five, have adequate bioavailability (score ~0.55), and show no anticipated AMES toxicity, indicating a satisfactory safety profile. Mechanistically, these benzoxazine derivatives decrease tumour cell proliferation and promote death by targeting CDK9, a crucial regulator of transcriptional elongation implicated in oncogene expression (such as MYC and MCL-1). Overall, the combined in silico results show that Compound 6 is a promising lead candidate for additional in vitro and in vivo testing as a possible anticancer drug, followed by Compounds 4, 1, and 3.[23]

4. CONCLUSION

This study successfully employed computational methods to evaluate a series of 10 novel benzoxazine derivatives as potential CDK9 inhibitors. Several drugs outperform the conventional inhibitor CDK9-IN-23 in terms of binding affinity, according to molecular docking against the CDK9 active site (PDB ID: 6GHZ). With a docking score of −9.0 kcal/mol, compound 6 proved to be the most effective candidate, forming crucial contacts with LYS75, GLN72, and

ILE85. Additionally, Lipinski's Rule of Five is closely followed by the top leads, which have great theoretical bioavailability and no AMES toxicity, according to predicted ADME profiling. These results imply that halogenated benzoxazine scaffolds are extremely attractive and practical candidates for the creation of targeted treatments for CDK9-driven cancers. To verify these reliable in silico predictions experimentally, more in vivo research and in vitro enzymatic tests are necessary.

REFERENCES

1. J. Petronijević, et al., biological evaluation of selected 3,4-dihydro-2(1H) quinoxalinones and 3,4-dihydro-1,4-benzoxazin-2-ones: Molecular docking study, J. Mol. Struct. 130959 (2021).
2. G.P. Gregory, S.J. Hogg, L. Kats, Dual inhibition of CDK9 and MYC as a therapeutic strategy in cancer, Leukaemia, 2022; 1–12.
3. C.H. Huang, et al., CDK9-mediated transcription elongation is required for MYC addiction and tumorigenesis, Proc. Natl. Acad. Sci. U.S.A., 2014; 111(30): 3150–3159.
4. R. Mandal, S. Becker, K. Strebhardt, Targeting CDK9 for anti-cancer therapeutics, Cancers, 2011; 3: 112–138.
5. S. Wang, P.M. Fischer, Targeting CDK9 for cancer therapy: mechanisms and advances, Nat. Rev. Drug Discov, 2023; 1–20.
6. T. Song, et al., Synthesis and evaluation of a 3,4-dihydro-2H-benzoxazine derivative as 51 a potent CDK9 inhibitor for anticancer therapy, J. Med. Chem, 2017; 60: 10092– 10108.
7. H. Patel, M. Periyasamy, G.P. Sava, CDK9 inhibitors in cancer: current perspectives and future directions, J. Med. Chem, 2022; 7350–7372.
8. L.D. Mendelsohn, ChemDraw 8 Ultra, Windows and Macintosh versions, J. Chem. Inf. Computer. Sci., 2004.
9. Mendelsohn, L. D. Chem Draw 8 Ultra, Windows and Macintosh Versions, Journal of Chemical Information and Computer Sciences, 2004. ([ACS Publications]
10. Trott O, Olson AJ. AutoDock Vina: improving the speed and accuracy of docking with a new scoring function, efficient optimization, and multithreading. J Computer Chem, 2010; 31(2): 455–461.
11. O'Boyle, N. M. et al. *"Open Babel: An open chemical toolbox", *Journal of Cheminformatics, 2011. ([SpringerLink]
12. Daina, O. Michielin, V. Zoete, SwissADME: A free web tool to evaluate pharmacokinetics, drug-likeness and medicinal chemistry friendliness of small molecules, Sci. Rep., 2017; 7: 42717.
13. SwissADME Official Website (https://www.swissadme.ch)
14. Schrödinger, LLC., The PyMOL Molecular Graphics System, 2015.
15. DeLano, W. L., PyMOL: An Open-Source Molecular Graphics Tool, 2002.
16. C.M. Olson, et al., Pharmacological perturbation of CDK9 using selective inhibitors suppresses transcriptional elongation in cancer, Cancer Cell, 2018; 34(5): 792–805.
17. G.E. Winter, et al., BET bromodomain proteins function as master transcription elongation factors independent of CDK9, Cell, 2017; 168(5): 896–909.
18. R. Chen, et al., CDK9 inhibition strategy defines a therapeutic window in MYC-driven cancers, Nat. Commun, 2019; 10: 531.
19. H. Zhang, et al., Design, synthesis, and biological evaluation of benzoxazine derivatives as anticancer agents, Eur. J. Med. Chem, 2020; 207: 112742.

20. S. Boffo, et al., Structure-based drug design targeting CDK9: recent advances, Drug Discov. Today, 2021; 26(6): 1432–1442.
21. S. Diab, et al., Benzoxazine derivatives as emerging scaffolds in medicinal chemistry, Bioorg. Med. Chem. Lett., 2022; 58: 128529.
22. X. Li, et al., Advances in targeting transcriptional CDKs for cancer therapy, Trends Pharmacology. Sci., 2023; 44(2): 98–112.
23. N. Kwiatkowski, et al., Targeting transcription regulation in cancer with CDK inhibitors, Nature, 2014; 511: 616–620.